



Pergamon

SCIENCE @ DIRECT®

Bioorganic & Medicinal Chemistry 11 (2003) 5259–5272

BIOORGANIC &  
MEDICINAL  
CHEMISTRY

# High Affinity Central Benzodiazepine Receptor Ligands. Part 3: Insights Into the Pharmacophore and Pattern Recognition Study of Intrinsic Activities of Pyrazolo[4,3-*c*]quinolin-3-ones<sup>†</sup>

Andrea Carotti,<sup>a</sup> Cosimo Altomare,<sup>a,\*</sup> Luisa Savini,<sup>b</sup> Luisa Chiasserini,<sup>b</sup>  
Cesare Pellerano,<sup>b</sup> Maria P. Mascia,<sup>c</sup> Elisabetta Maciocco,<sup>c</sup> Fabio Busonero,<sup>c</sup>  
Manuel Mameli,<sup>c</sup> Giovanni Biggio<sup>c</sup> and Enrico Sanna<sup>c</sup>

<sup>a</sup>Dipartimento Farmaco Chimico, Università degli Studi, Via E. Orabona 4, I-70125 Bari, Italy

<sup>b</sup>Dipartimento Farmaco Chimico Tecnologico, Università degli Studi, Via A. Moro, I-53100 Siena, Italy

<sup>c</sup>Dipartimento di Biologia Sperimentale, Università degli Studi, Via Palabanda 12, I-09123 Cagliari, Italy

Received 3 January 2003; accepted 29 July 2003

**Abstract**—Novel 2-phenyl-2,5-dihydropyrazolo[4,3-*c*]quinolin-3-(3*H*)-ones (PQs) endowed with high affinity for central benzodiazepine receptor (BzR) were synthesized. In particular, 9-fluoro-2-(2-fluorophenyl)-2,5-dihydro-3*H*-pyrazolo[4,3-*c*]quinolin-3-one (**2**) showed binding affinity in the subnanomolar concentration range and proved to be in vitro a potent antagonist. This finding allowed the nature of the hydrogen bonding receptor site H<sub>2</sub> to be established, as located between the N-1 nitrogen of the PQ nucleus and the *ortho* position of the N-2-aryl group. [<sup>35</sup>S]*tert*-Butylbicyclophosphorothionate ([<sup>35</sup>S]TBPS) binding assays and electrophysiological measurements of the effects on GABA-evoked Cl<sup>−</sup> currents at recombinant human  $\alpha_1\beta_2\gamma_{2L}$  GABA<sub>A</sub> receptors, expressed in *Xenopus laevis* oocytes, were used to assess the intrinsic activities of a large series of PQs. With the aim of extracting discriminant information and distinguishing BzR ligands with different profiles of efficacy, 51 PQ derivatives, including full and partial agonists, antagonists, and inverse agonists, were analyzed in a multidimensional chemical descriptor space, defined by the lipophilicity parameter CLOG P and 3-D molecular WHIM descriptors, by means of principal component analysis, *k*-nearest neighbors (*k*-NN) method, and linear discriminant analysis (LDA). The classification methods were applied to subsets of pairs of efficacy classes, and lipophilicity and 3-D size descriptors were detected as the discriminant variables by a stepwise linear discriminant analysis. LDA proved to be superior to *k*-NN, especially in classifying PQ ligands (60–84% of success in prediction ability) into categories of efficacies which were contiguous and quite overlapped in the hyperspace of variables.

© 2003 Elsevier Ltd. All rights reserved.

## Introduction

The mechanisms responsible for the biological action of ligands at the benzodiazepine receptor (BzR) have been the object of an intensive inquiry during the last three decades.<sup>1</sup> BzR is coupled to the  $\gamma$ -aminobutyric acid (GABA) receptor and is a part of GABA<sub>A</sub>-controlled chloride ion channel (BzR/GABA<sub>A</sub>/Cl<sup>−</sup>) complex. Indeed, BzR ligands, either benzodiazepines (Bz) or structurally unrelated compounds, act as modulators of

GABA binding to its receptor, by altering the trans-membrane chloride ion conductance.<sup>2,3</sup>

GABA<sub>A</sub>/BzR complex is a membrane-bound heteropentameric protein constituted by different subunits. A total of 21 subunits (6 $\alpha$ , 4 $\beta$ , 4 $\gamma$ , 1 $\epsilon$ , 1 $\delta$ , 3 $\rho$ , 1 $\vartheta$  and 1 $\pi$ ) have been identified by molecular cloning,<sup>4</sup> and 16 of them have been found in the mammalian CNS.<sup>5</sup> It has been shown that a functional GABA<sub>A</sub>/BzR must contain  $\alpha$ ,  $\beta$  and  $\gamma$  subunits.

The great interest toward BzR ligands stem from their ability to induce different central effects, depending on their intrinsic activity profile (positive, negative, and zero efficacy at the GABA<sub>A</sub> receptor). In a *continuum* of intrinsic activities, BzR ligands can range from full agonism through antagonism to inverse agonism.<sup>6–10</sup>

\*Corresponding author. Tel.: +39-080-544-2781; fax: +39-080-544-2230; e-mail: altomare@farmchim.uniba.it

<sup>†</sup>This paper is dedicated to the memory of Prof. Cesare Pellerano, who died 10 August 2003. In him we have lost a colleague with high-scientific and humane qualities, who has greatly contributed to research on the medical chemistry of quinoline-containing compounds.

Full agonists (*Ag*) elicit sedative, amnesic, anxiolytic, anticonvulsant effects, as well as ataxia, alcohol potentiation and muscle relaxant properties. Full inverse agonists (*IA*) exert a negative cooperative effect on GABA binding to its receptor complex, resulting in mirror image biological effects over the full agonists (e.g., anxiogenic, proconvulsant, cognition enhancement, reversal of alcohol effects). Antagonists (*An*), which are characterized by nil efficacy on the normal GABA<sub>A</sub>/Cl<sup>−</sup> channel function, display no relevant effects of their own other than a selective blockade of the effects of both agonists and inverse agonists.<sup>11</sup> Diazepam, ethyl ester of  $\beta$ -carbolin-3-carboxylic acid ( $\beta$ -CCE), and Ro 15-1788 (an imidazolbenzodiazepine derivative) are typical representatives of an agonist, an inverse agonist and an antagonist, respectively (Fig. 1).

Within classes of BzR ligands, compounds having minor structural modifications and similar binding interactions (IC<sub>50</sub>) can display activities across the full spectrum from agonist to antagonist and inverse agonist. The notion of partial agonists (*PA*) and inverse agonists (*PIA*) has been also introduced. Among partial agonists, compounds have been reported that exhibit in vivo anxiolytic with no anticonvulsant properties, anxiolytic/anticonvulsant activities without other effects associated with compounds that bind BzR, and muscle relaxant but not anxiolytic and anticonvulsant effects.<sup>12–14</sup> Even more importantly, due to prevailing adverse biological effects of the full *IA* ligands of BzR (e.g., anxiogenic, convulsant), compounds having a therapeutic potential might be obtained from partial inverse agonists (*PIA*).<sup>11</sup>

The heterogeneity of GABA<sub>A</sub>/BzR subtypes has been indicated as a major cause of the multiplicity of the pharmacological properties displayed by BzR ligands.<sup>15</sup> A direct relationship between the observed pharmacological activities and the different receptor subtypes has not been established yet, even though recently, based on data obtained using alpha-subunit knock-in mice, it has been suggested that specific GABA<sub>A</sub> receptor subtypes mediate specific benzodiazepine-induced behavioral effects.<sup>16–19</sup>

Among the diverse compounds that selectively bind to the GABA<sub>A</sub>/BzR complex, 2-aryl-2,5-dihydropyrazolo[4,3-*c*]quinoline-3-(3*H*)ones (PQs), well-established high-affinity ligands of the central BzR, have been recently investigated by some of us. PQ BzR-ligands are lacking of many unwanted side effects associated to the administration of classical benzodiazepines, and display different intrinsic activities, even upon small chemical variations.<sup>20–24</sup> Our previous studies on synthesis, bind-

ing, SARs and three-dimensional quantitative SARs (3-D QSARs) have allowed the existing pharmacophores<sup>25–27</sup> to be usefully integrated<sup>28</sup> and Comparative Molecular Field Analysis (CoMFA) models to be generated.<sup>29</sup> As an useful integration of the pharmacophore, compelling computational evidence (ab initio calculations of molecular electrostatic potential, MEP) has been very recently brought that identifies a three-centered hydrogen bond (HB) at the HB donor site H<sub>2</sub>, suitably located in proximity of the N-1 and the N'-1 heterocyclic nitrogen or the fluorine atom at the C-2' position of the N-2 phenyl ring, as a key interaction for high receptor binding affinity.

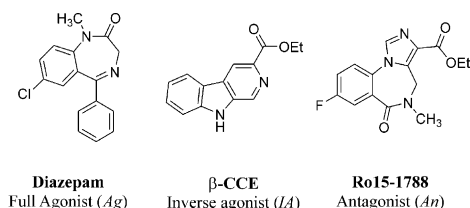
With the aim of gaining further proofs of the role of a HB involving F-C, the so-called 'organic fluorine',<sup>30–32</sup> as an acceptor in the molecular recognition of PQ ligands by the central BzRs, we synthesized two novel fluoro-PQ derivatives, namely 9-fluoro-2-phenyl-2,5-dihydro-3*H*-pyrazolo[4,3-*c*]quinolin-3-one (**2**<sub>1</sub>) and its 2-(2-fluorophenyl) congener (**2**<sub>2</sub>), and studied their in vitro pharmacology in depth.

Although a large number of PQ-containing BzR ligands are known, at the best of our knowledge no patterns have yet emerged which can allow PQ ligands with predictable intrinsic activities to be rationally designed. A second goal of this work was the investigation of the structure–efficacy relationships. Estimates of the intrinsic activities of more than 50 molecular variants of PQs, mostly bearing substituents at C-8 of the quinoline moiety and *para*-substituted phenyl or nitrogen heterocycle groups at N-2 of the pyrazole ring (Table 1), were obtained using a binding assay with [<sup>35</sup>S]TBPS,<sup>33,34</sup> and electrophysiological measurements on the cloned receptor subtype  $\alpha_1\beta_2\gamma_2L$ ,<sup>35</sup> which is the most abundant one in the CNS (ca. 45% of all GABA<sub>A</sub> receptors) and possesses the optimal and classical sensitivity for most of known GABAergic drugs. Feature selection and pattern recognition techniques were applied to such a set of ligands with different intrinsic activities (*Ag*, *PA*, *An*, and *IA*), each compound being described by a lipophilicity parameter (calculated octanol–water partition coefficient, CLOG P)<sup>36</sup> and 3-D molecular indices, namely Weighted Holistic Invariant Molecular (WHIM) descriptors.<sup>37,38</sup> Principal Component Analysis (PCA), and two classification methods, one non-parametric (*k* nearest neighbours, *k*-NN)<sup>39</sup> and one parametric (Linear Discriminant Analysis, LDA),<sup>40</sup> were applied in order to find molecular features that at best discriminate between ligands with different efficacy profiles and develop classification models usable in drug design.

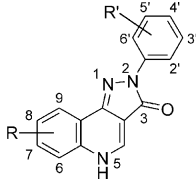
## Chemistry

2,5-Dihydro-3*H*-pyrazolo[4,3-*c*]quinolin-3-one derivatives (PQs, **2**) were synthesized through the general procedure shown in Scheme 1, using methods previously reported.<sup>28,29,41–43</sup>

The reaction of appropriate ethyl 4-chloro-quinoline-3-carboxylates with phenylhydrazines or  $\alpha$ -(*N*)-hetero-



**Figure 1.** Structure of known BzR ligands with well-established efficacy profiles.

**Table 1.** Binding data, in vitro efficacy profiles and lipophilicity of pyrazolo[4,3-*c*]quinolin-3-ones


Compd	set	<i>R</i> <sub>6</sub>	<i>R</i> <sub>7</sub>	<i>R</i> <sub>8</sub>	<i>R</i> <sub>9</sub>	<i>R</i> <sub>2'</sub>	<i>R</i> <sub>3'</sub>	<i>R</i> <sub>4'</sub>	pIC <sub>50</sub> <sup>a</sup>	Efficacy <sup>b</sup>	CLOG P <sup>c</sup>
Compounds used for LDA model derivation (Ts = Test set; all the others in the Training set)											
23 <sup>d</sup>		H	H	cC <sub>6</sub> H <sub>11</sub>	H	H	H	H	8.35	Ag	5.52
24		H	H	<i>n</i> .C <sub>4</sub> H <sub>9</sub>	H	F	H	H	9.18	Ag	5.13
25 <sup>d</sup>	Ts	H	H	<i>n</i> .C <sub>4</sub> H <sub>9</sub>	H	H	H	H	9.00	Ag	4.98
26		H	H	<i>n</i> .C <sub>4</sub> H <sub>9</sub>	H	H	H	COOCH <sub>3</sub>	6.86	Ag	4.95
27		H	H	OCF <sub>3</sub>	H	H	H	Br	7.82	Ag	4.81
28		H	H	OCF <sub>3</sub>	H	H	H	Cl	7.90	Ag	4.66
29		H	H	OC <sub>4</sub> H <sub>9</sub>	H	F	H	H	9.08	Ag	4.57
210		H	H	OC <sub>4</sub> H <sub>9</sub>	H	H	H	H	8.54	Ag	4.42
211		H	H	OCF <sub>3</sub>	H	H	F	H	9.40	Ag	4.09
212		H	H	OCF <sub>3</sub>	H	H	H	F	9.00	Ag	4.09
213	Ts	H	H	OC <sub>2</sub> H <sub>5</sub>	H	H	H	Cl	8.56	Ag	4.08
214		H	H	OCF <sub>3</sub>	H	H	H	H	9.15	Ag	3.94
215		F	F	F	H	H	H	Cl	7.13	Ag	3.92
216		H	H	OCF <sub>3</sub>	H	H	H	OCH <sub>3</sub>	9.22	Ag	3.87
217	Ts	H	H	<i>n</i> .C <sub>4</sub> H <sub>9</sub>	H		2-Pyrid-2'-yl		9.50	Ag	3.49
218	Ts	H	H	cC <sub>6</sub> H <sub>11</sub>	H		2-Pyrazin-2'-yl		8.16	Ag	3.06
219 <sup>c</sup>		H	H	H	H	H	H	H	9.35	Ag	2.90
220		H	H	OCF <sub>3</sub>	H	H	H	N(CH <sub>3</sub> ) <sub>2</sub>	8.26	PA	4.11
221		H	H	OCF <sub>3</sub>	H	F	H	H	9.40	PA	4.09
222 <sup>f</sup>	Ts	F	H	F	H	H	H	Br	6.79	PA	4.07
223		H	H	cC <sub>6</sub> H <sub>11</sub>	H		2-Pyrid-2'-yl		8.60	PA	4.03
224		H	H	OCF <sub>3</sub>	H	H	H	NO <sub>2</sub>	7.40	PA	3.69
225 <sup>e</sup>		H	H	H	H	H	H	Cl	9.00	PA	3.61
226		H	H	OCF <sub>3</sub>	H	H	H	OH	9.63	PA	3.29
227	Ts	F	F	F	H	H	H	H	7.70	PA	3.21
228 <sup>f</sup>		F	H	F	H	H	H	OCH <sub>3</sub>	8.12	PA	3.13
229	Ts	H	H	cC <sub>6</sub> H <sub>11</sub>	H		2-Pyrimid-2'-yl		8.36	PA	3.06
230		H	H	OH	H	H	H	Cl	9.28	PA	2.97
231 <sup>e</sup>		H	H	OCH <sub>3</sub>	H	H	H	H	9.17	PA	2.84
232		H	H	OCF <sub>3</sub>	H	H	H	NH <sub>2</sub>	9.10	PA	2.73
233		H	H	<i>n</i> .C <sub>4</sub> H <sub>9</sub>	H		2-Pyrazin-2'-yl		9.22	PA	2.53
234		H	H	OCF <sub>3</sub>	H	H	NH <sub>2</sub>	OH	7.98	PA	2.43
235		H	Cl	H	H	H	H	H	8.67	An	3.63
236		H	H	OCF <sub>3</sub>	H		2-Pyrid-2'-yl		1.35	An	2.45
237		H	H	OH	H	F	H	H	8.88	An	2.40
238	Ts	H	7.8-OCH <sub>2</sub> O		H	H	H	H	8.52	An	2.33
239		H	7.8-OCH <sub>2</sub> O		H	H	H	OCH <sub>3</sub>	8.14	An	2.25
240		H	H	OH	H	H	H	H	9.70	An	2.25
241		H	H	H	H	H	H	OH	9.40	An	2.25
242		H	OCH <sub>3</sub>	OCH <sub>3</sub>	OCH <sub>3</sub>	H	H	H	8.90	An	2.00
243		H	NH <sub>2</sub>	H	H	H	H	H	8.86	An	1.69
244		H	H	H	H	H	H	NH <sub>2</sub>	8.67	An	1.69
245	Ts	F	H	F	H		2-Pyrazin-2'-yl		6.94	An	0.75
246		H	OCH <sub>3</sub>	H	H	H	H	H	8.37	IA	2.84
247		H	OH	H	H	H	H	H	8.88	IA	2.25
248		H	H	Cl	H		2-Pyrid-2'-yl		9.37	IA	2.13
249	Ts	F	H	F	H		2-Pyrid-2'-yl		7.82	IA	1.71
250		H	H	OCF <sub>3</sub>	H		2-Pyrimid-2'-yl		8.50	IA	1.49
251		H	H	OCF <sub>3</sub>	H		2-Pyrazin-2'-yl		8.96	IA	1.49
252		H	H	OH	H		2-Pyrid-2'-yl		7.75	IA	0.76
253	Ts	H	OCH <sub>3</sub>	OCH <sub>3</sub>	OCH <sub>3</sub>		2-Pyrazin-2'-yl		8.94	IA	-0.45
Compounds used for prediction											
21		H	H	H	F	H	H	H	8.48	An	3.06
22		H	H	H	F	F	H	H	9.68	An	3.20
Compounds left out from the classification analysis											
254 <sup>c</sup>		H	H	Cl	H	H	H	H	9.37	Mixed	3.63
255 <sup>f</sup>		F	H	F	H	H	F	H	8.02	Mixed	3.35
256 <sup>g</sup>				H	H	H	H	2-Pyrid-2'-yl	9.21	Mixed	1.41
257		H	H	OCH <sub>3</sub>	H		2-Pyrid-2'-yl		9.10	Mixed	1.94
258		H	H	OCH <sub>3</sub>	H		2-Pyrimid-2'-yl		8.89	Mixed	0.38

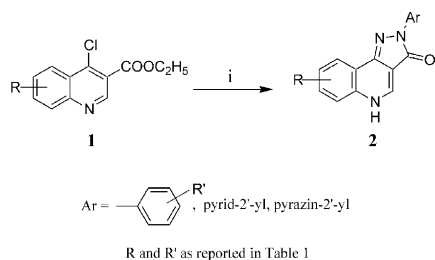
<sup>a</sup>Binding data from the displacement of [<sup>3</sup>H]-flunitrazepam.<sup>b</sup>Efficacy profile (see text for definition); Ag, agonist; PA, partial agonist; An, antagonist; IA, inverse agonist.<sup>c</sup>Compounds are ordered along a decreasing value of calculated octanol–water partition coefficient (CLOG P) within each group of efficacy category.<sup>d</sup>Ref 41.<sup>e</sup>Refs 22 and 23; IC<sub>50</sub> value of compound 225 (CGS-9896), used as reference standard, has been redetermined in this study.<sup>f</sup>Ref 42.<sup>g</sup>Ref 44.

cyclic hydrazines afforded the desired PQs in satisfactory yields. 9-Fluoro-2-phenyl-2,5-dihydro-3*H*-pyrazolo[4,3-*c*]quinolin-3-one (**2**<sub>1</sub>), its 2-(2-fluorophenyl) congener (**2**<sub>2</sub>), and PQs **2**<sub>37</sub>, **2**<sub>51</sub>, **2**<sub>52</sub>, **2**<sub>57</sub> are novel, whereas one compound had been already described in patent literature (**2**<sub>56</sub>).<sup>44</sup> The hydroxy derivatives (**2**<sub>37</sub>, **2**<sub>52</sub>) were conveniently obtained from the corresponding alkoxyderivatives by hydrolysis with 48% HBr in glacial acetic acid, as already described.<sup>28</sup> Physicochemical properties and spectroscopic data of newly synthesized compounds are reported in the experimental section (Tables 5 and 6).

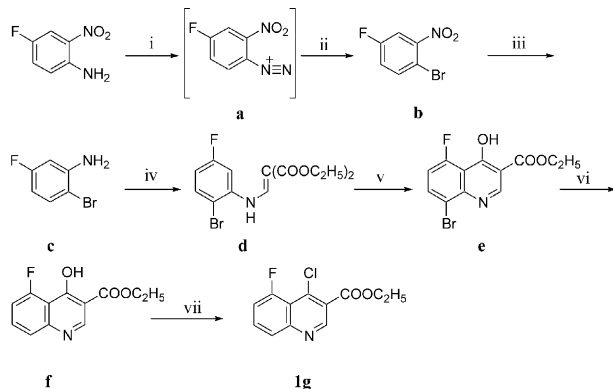
IR and <sup>1</sup>H NMR data, in full agreement with the literature, allowed us unequivocal structural assignment of all new compounds. In <sup>1</sup>H NMR spectra, the characteristic signals for PQs were a singlet between 8.5 and 8.9 δ assigned to H-4, and a broad singlet, exchangeable with D<sub>2</sub>O, between 12.6 and 13.1 δ assigned to the N<sub>5</sub>-H proton. As for compound **2**<sub>2</sub> due to a possible tautomeric equilibrium, the H-4 proton appeared as a doublet that collapsed to a singlet upon treatment with D<sub>2</sub>O.

The known CGS-8216 and CGS-9896 (**2**<sub>19</sub> and **2**<sub>25</sub>, respectively, in Table 1) were also synthesized<sup>43</sup> and tested in this study.

The synthetic pathway for preparing the unknown ethyl 4-chloro-5-fluoroquinoline-3-carboxylate (**1g**), used as starting material for the synthesis of compounds **2**<sub>1</sub> and **2**<sub>2</sub> is illustrated in Scheme 2.



**Scheme 1.** (i) R'-phenylhydrazine, EtOH, reflux, or 2-hydrazinopyrazine-, 2-hydrazinopyridine, rt.



**Scheme 2.** Reagents and conditions: (i) HCl concn, 5M NaNO<sub>2</sub> (aqueous solution), 0 °C; (ii) CuBr, HCl concn, 0 °C, then 60 °C for 3 h; (iii) Ni Raney, H<sub>2</sub>; (iv) diethylethoxymethylene malonate, steam bath; (v) diphenyl ether, reflux; (vi) AcOH, AcONa, Pd/C 10%, H<sub>2</sub>; (vii) POCl<sub>3</sub>, sand bath.

Diazotization and subsequent displacement of diazonium salt with CuBr on 2-nitro-4-fluoroaniline led to the intermediate **b**,<sup>45</sup> that was reduced with H<sub>2</sub> and Raney Ni as catalyst to give the aniline intermediate **c**.<sup>46</sup> Condensation of **c** with diethyl ethoxymethylenemalonate afforded compound **d**, which via thermal ring closure in boiling diphenyl ether gave ethyl 8-bromo-5-fluoro-4-hydroxyquinoline-3-carboxylate **e**. Debromination by hydrogenolysis with Pd/C afforded **f**, and treatment of **f** with phosphorus oxychloride led to the desired derivative **1g**.

## Biochemistry and Electrophysiology

### Fluoro derivatives of pyrazolo[4,3-*c*]quinolin-3-one

In order to evaluate the affinity of the novel fluoro derivatives, **2**<sub>1</sub> and **2**<sub>2</sub>, for the BzR at the GABA<sub>A</sub> receptor complex, [<sup>3</sup>H]flunitrazepam binding was performed in rat brain homogenates, and their effects were compared to that produced by the reference standard CGS-9896 (**2**<sub>25</sub>). Compounds **2**<sub>1</sub> and **2**<sub>2</sub> were able to completely displace the binding of [<sup>3</sup>H]flunitrazepam with IC<sub>50</sub> values of 3.3 nM for compound **2**<sub>1</sub> and 0.21 nM for compound **2**<sub>2</sub>. The IC<sub>50</sub> value for CGS-9896 (**2**<sub>25</sub>) determined in the same assay was 1 nM.

The modulatory action of these compounds on GABA-evoked Cl<sup>-</sup> was determined by electrophysiological recordings performed in *Xenopus laevis* oocytes expressing recombinant GABA<sub>A</sub> receptors composed of α<sub>1</sub>, β<sub>2</sub>, and γ<sub>2L</sub> subunits. This functional assay revealed that neither **2**<sub>1</sub> nor **2**<sub>2</sub>, at any of the concentrations tested (0.001–10 μM), altered the response to an EC<sub>5-10</sub> concentration of GABA (Fig. 2). By comparison, CGS-9896 increased (69 ± 13%) GABA-evoked Cl<sup>-</sup> currents only at the highest concentration (10 μM) tested, whereas diazepam, as expected, markedly and concentration-dependently potentiated (102 ± 8%) the action of GABA with an EC<sub>50</sub> of 0.17 μM.

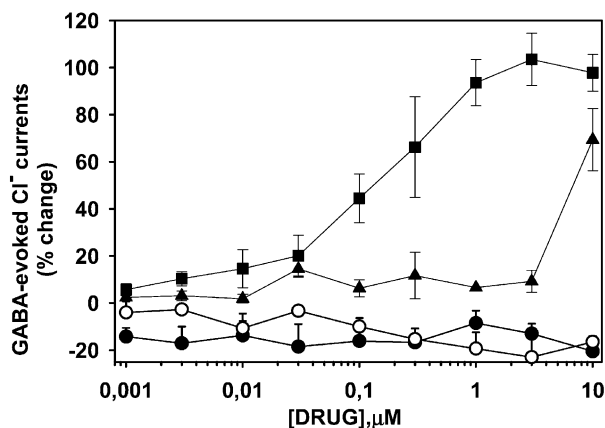


**Figure 2.** Effects of **2**<sub>1</sub> and **2**<sub>2</sub> (0.001–10 μM) on recombinant α<sub>1</sub>β<sub>2</sub>γ<sub>2L</sub> GABA<sub>A</sub> receptors expressed in *Xenopus laevis* oocytes. **2**<sub>1</sub> (closed circle), **2**<sub>2</sub> (open circle), **2**<sub>25</sub> CGS-9896 (closed triangles), or diazepam (closed squares) were preapplied for 1 min before being coapplied for 30 s with an EC<sub>5-10</sub> of GABA (6–10 μM). Data are the mean ± SEM (*n* = 4–5).

However, in line with expectations from the [ $^3\text{H}$ ]flunitrazepam binding assays, Figure 3 shows that both **2<sub>1</sub>** and **2<sub>2</sub>** (0.001–3  $\mu\text{M}$  dosing range) reduced in a concentration-dependent manner the effect on  $\alpha_1\beta_2\gamma_{2\text{L}}$  GABA<sub>A</sub> receptor function induced by diazepam at 1  $\mu\text{M}$  concentration, which per se markedly potentiated the response to GABA ( $\sim +95\%$  vs control responses), the estimated  $\text{IC}_{50}$  values (i.e., the concentration required to halve the effect of diazepam) being approximately 1 and 1.5 nM for **2<sub>1</sub>** and **2<sub>2</sub>**, respectively.

#### Assessment of intrinsic activities of a large series of pyrazolo[4,3-*c*]quinolin-3-ones

The compounds listed in Table 1 were tested for their ability to displace [ $^3\text{H}$ ]flunitrazepam binding from rat brain membranes according to standard procedures.<sup>33</sup> The  $\text{pIC}_{50}$  values reported in Table 1 have been normalized using CGS-9896 (**2<sub>25</sub>**) as the reference standard.

The efficacy profiles for all the PQ derivatives under examination were assessed using the binding assay with [ $^{35}\text{S}$ ]TBPS, which proved a biochemical tool better than the method based on the determination of the GABA ratio (i.e.,  $\text{IC}_{50}$  without GABA/ $\text{IC}_{50}$  with GABA) in evaluating in vitro the intrinsic activities of both positive and negative modulators of GABA<sub>A</sub> receptor complex.<sup>47</sup> Accordingly, full agonists decrease the specific [ $^{35}\text{S}$ ]TBPS binding in a dose-dependent manner, whereas full inverse agonists show opposite effects.<sup>48,49</sup> In contrast, no significant effects are observed with antagonists. The results obtained with nine PQ ligands, displaying different behaviors in the [ $^{35}\text{S}$ ]TBPS binding assay, are graphically shown in Figure 4. Most of the PQ ligands tested (45 out of 56 compounds) showed undoubtful intrinsic activities.

In order to better characterize the profile of eleven compounds, behaving as mixed forms or showing doubtful results in the [ $^{35}\text{S}$ ]TBPS binding assay, we investigated their modulation of GABA-evoked chloride currents by electrophysiological measurements on

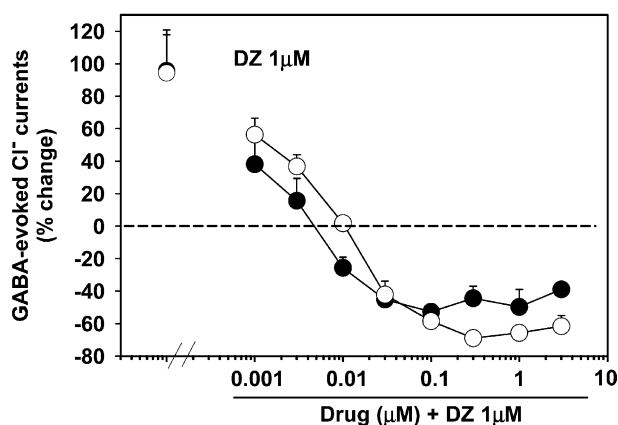


**Figure 3.** Compounds **2<sub>1</sub>** and **2<sub>2</sub>** (0.001–3  $\mu\text{M}$ ) antagonize the effect of diazepam (1  $\mu\text{M}$ ) in recombinant  $\alpha_1\beta_2\gamma_{2\text{L}}$  GABA<sub>A</sub> receptors expressed in *Xenopus laevis* oocytes. **2<sub>1</sub>** (closed circle) or **2<sub>2</sub>** (open circle) were preapplied for 1 min before being coapplied for 30 s with an  $\text{EC}_{5-10}$  of GABA (6–10  $\mu\text{M}$ ). Data are the mean  $\pm$  SEM ( $n=4-5$ ).

cloned human GABA<sub>A</sub> receptor subunit constructs ( $\alpha_1\beta_2\gamma_{2\text{L}}$ ) in *Xenopus laevis* oocytes. Together with these compounds, 19 PQ derivatives, chosen as representative of the 45 compounds which displayed defined intrinsic activities in the above assay, were also investigated through the electrophysiological measurements, in order to evaluate the reliability of the assignment of efficacy category based on these two experimental in vitro models. For each investigated PQ ligand, modulatory effects on GABA-evoked  $\text{Cl}^-$  currents at  $\alpha_1\beta_2\gamma_{2\text{L}}$  GABA<sub>A</sub> receptors were measured at two compound concentrations (1 and 10  $\mu\text{M}$ ). The results obtained are shown in Figure 5 for the same set of compounds reported in Figure 4, in order to allow a direct comparison between profiles determined by the two assays. Looking at the results shown in Figures 4 and 5, it appears that, with two exceptions (i.e., **2<sub>42</sub>** which displayed an *IA* profile in the [ $^{35}\text{S}$ ]TBPS binding assay whereas behaved as an *An* in the electrophysiological assay; **2<sub>49</sub>** showed a clear *IA* behavior in the electrophysiological assay in contrast with the *An* profile inferred by the [ $^{35}\text{S}$ ]TBPS binding assay), the two assays gave similar results. Moreover, the in vitro experimental models adopted in this study resulted in a fully convergent assignment of efficacy

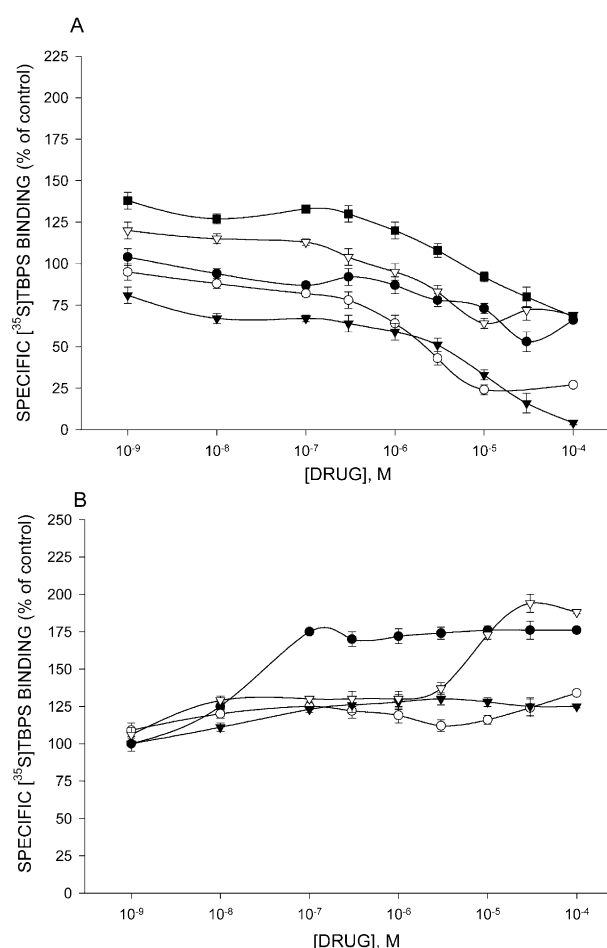


**Figure 4.** Effects of modulation of some PQs and the reference standard CGS-9896 on [ $^{35}\text{S}$ ]TBPS binding in rat cerebral cortex. Data are expressed as percentage of control. Each value is the mean  $\pm$  SEM of three independent experiments performed in triplicate. Symbols: (A) **2<sub>4</sub>** ( $\blacktriangledown$ ), **2<sub>13</sub>** ( $\circ$ ), **2<sub>20</sub>** ( $\blacksquare$ ), **2<sub>21</sub>** ( $\nabla$ ), **2<sub>25</sub>** ( $\bullet$ ); (B) **2<sub>42</sub>** ( $\bullet$ ), **2<sub>45</sub>** ( $\circ$ ), **2<sub>47</sub>** ( $\nabla$ ), **2<sub>49</sub>** ( $\blacktriangledown$ ).



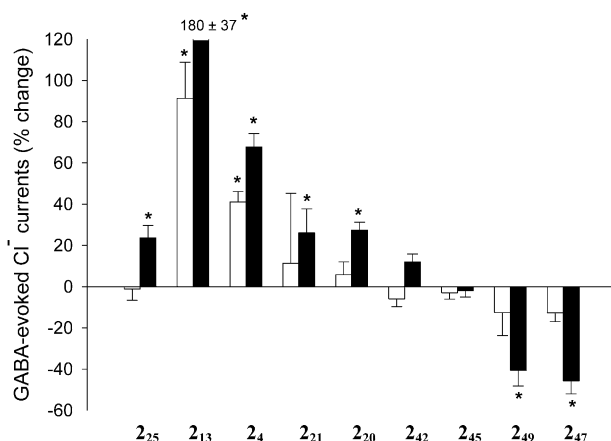


**Figure 5.** Effects of PQs (1  $\mu$ M concentration, open bars; 10  $\mu$ M concentration, closed bars) on GABA-evoked  $\text{Cl}^-$  currents at human  $\text{GABA}_A$  receptors. *Xenopus* oocytes expressing  $\alpha_1$ ,  $\beta_2$ , and  $\gamma_{2L}$  subunits of human  $\text{GABA}_A$  receptors were voltage-clamped at  $-70$  mV in order to measure  $\text{Cl}^-$  currents evoked by GABA. Data are expressed as percent change relative to the control response elicited by GABA alone and are means  $\pm$  SEM ( $n=4-5$ ). \* $p \leq 0.05$  versus the control response.

profiles for more than 80% of the 19 PQ derivatives taken as an internal control set (i.e., the compounds displaying well-defined behaviors in the [ $^{35}\text{S}$ ]TBPS binding assay), most of the different assignments being observed for contiguous efficacy profiles (*Ag-PA*, *PA-An*, *An-IA*).

Taking all the above in mind, the efficacy profiles were finally assigned (Table 1) according to the following criteria: (i) due to the largest availability of data, the results from [ $^{35}\text{S}$ ]TBPS binding studies had priority; (ii) for [ $^{35}\text{S}$ ]TBPS efficacy profiles of difficult interpretation (e.g., borderline behavior between contiguous efficacy profiles: *Ag-PA*, *PA-An*, *An-IA*), electrophysiological measurements using cloned human  $\text{GABA}_A$  receptors ( $\alpha_1\beta_2\gamma_{2L}$ ) were taken into account in order to accomplish the assignment; thus, for example, a compound showing a behavior borderline between partial agonism and antagonism was assigned to *PA* or *An* category, based on the observations made in the electrophysiological assay on cloned receptors; (iii) PQ ligands showing a doubtful behavior in [ $^{35}\text{S}$ ]TBPS binding assay (e.g., *An-IA*) and a different profile in the electrophysiological assay were assigned as mixed forms and left out from the classification analysis (compounds **2<sub>54</sub>**, **2<sub>55</sub>**, **2<sub>56</sub>**, **2<sub>57</sub>**, **2<sub>58</sub>**); they should deserve further biological investigation.

## Results and Discussion

### Validating the BzR pharmacophore

A relevant goal of the present study was the evaluation of the importance in the molecular recognition of PQ derivatives by central BzR of a three-center HB at the  $\text{H}_2$  HB donor site of the pharmacophore. In a previous computational study,<sup>29</sup> based on ab initio calculation and comparison of MEP minima, 2'-F substituent at the N-2-phenyl ring, similarly to the N'-1 heterocyclic

nitrogen, was found to strengthen the MEP minimum located in proximity of the  $\text{H}_2$  pharmacophore site. 9-Fluoro-2-phenyl PQ (**2<sub>1</sub>**) and its 2-(2'-fluorophenyl) congener (**2<sub>2</sub>**) were tested in order to assess the effects on the binding of the two fluorines which are in position quite symmetrical to the  $\text{H}_2$  HB donor site.

Our biochemical data showed that the fluorine-containing PQ derivatives **2<sub>1</sub>** and **2<sub>2</sub>** competitively inhibit at low nanomolar and subnanomolar concentrations, respectively, the specific [ $^3\text{H}$ ]flunitrazepam binding to rat cortical membranes. Compound **2<sub>2</sub>**, bearing fluorines at the C-9 position of the PQ nucleus and C-2' position of the N-2-phenyl ring, showed a 5- and a 2-fold increase in binding affinity over the reference standard CGS-9896 (**2<sub>25</sub>**) and the unsubstituted PQ (CGS-8216, **2<sub>19</sub>**), respectively. Its affinity resulted significantly higher (more than one magnitude order) than that of the parent compound **2<sub>1</sub>**, that bears fluorine at only the position C-9 of the PQ nucleus, making clear that the presence of a fluorine at the C-2' position is responsible for the high affinity whereas 9-F appears to exert a lower influence. Other examples of such an *ortho*-fluorine-dependent increase of binding affinity could be inferred from our previous findings (Table 1, pairwise comparison of **2<sub>4</sub>** with **2<sub>5</sub>**, **2<sub>9</sub>** with **2<sub>10</sub>**, and **2<sub>14</sub>** with **2<sub>21</sub>**).

Electrophysiological assays clearly indicated that both **2<sub>1</sub>** and **2<sub>2</sub>** are not able to significantly alter GABA-evoked  $\text{Cl}^-$  currents, whereas both compounds, at concentrations as low as 0.1  $\mu\text{M}$ , completely reversed diazepam-induced potentiation of GABA-evoked  $\text{Cl}^-$  currents, suggesting that the fluoro-derivatives **2<sub>1</sub>** and **2<sub>2</sub>** are potent antagonists at the benzodiazepine recognition site.

### Multivariate data analysis of efficacy profiles

**Lipophilicity–efficacy relations.** In Table 1, together with binding data and efficacy profiles as estimated by in vitro assays, we reported log P values calculated by CLOG P program<sup>36</sup> as the lipophilicity parameters. PQ derivatives cover a wide range of lipophilicity (ca. 6 log units) and are ordered in Table 1 along a decreasing log P value in order to help one in revealing if and how the lipophilicity of a PQ ligand could affect its intrinsic activity. A preliminary analysis of the data revealed that the log P parameter sharply discriminates between the two classes of ligands located at the extremes of the *continuum* of intrinsic activities. Full agonists (*Ag*) are indeed the most lipophilic compounds, with log P values ranging from 2.9 (compd **2<sub>19</sub>**) to 5.5 (compd **2<sub>3</sub>**), whereas full inverse agonists (*IA*) are the most hydrophilic compounds, their log P values ranging from  $-0.45$  (compd **2<sub>53</sub>**) to 2.8 (compd **2<sub>46</sub>**). Partial agonists (*PA*), antagonists (*An*) and other mixed forms (mostly *An/IA*) cover log P ranges partially overlapped among themselves and to those of *Ag* and *IA*, but as a trend partial agonists are in the upper (log P > 2.4) lipophilicity range. However, the lipophilicity can not account alone for variations in intrinsic activities of PQ ligands. In Table 1, there are a number of isolipophilic positional isomers whose efficacy profiles change depending

upon substitution pattern. We draw attention, for instance, on the PQ 7 and 8 positional isomers: the 8-OMe PQ **2**<sub>31</sub> behaves as a *PA*, whereas the 7-OMe PQ **2**<sub>46</sub> is an *IA*; the 8-OH isomer **2**<sub>40</sub> is an *An*, whereas the 7-OH isomer **2**<sub>47</sub> behaves as an *IA*. Limited physico-chemical variation about substituents at C-6, C-7 and C-9 positions does not allow any significant trend to be established, whereas a shift from full toward partial agonism may also depend upon the substitution pattern at the N2-aryl group (see for example the isolipophilic N2-fluorophenyl derivatives **2**<sub>11</sub>, **2**<sub>12</sub>, **2**<sub>21</sub>, and the N2-diazine derivatives **2**<sub>18</sub> and **2**<sub>29</sub>).

**3-D descriptors.** To take such a substitution pattern into account we calculated 3-D descriptors. Information about the whole 3-D molecular structures of PQ ligands, in terms of size, shape, symmetry and atom distribution, was obtained by calculating WHIM<sup>37,38</sup> descriptors with DRAGON software (ver. 2.1).<sup>50</sup> Briefly, these indices are calculated by a principal component analysis (PCA) on the centered Cartesian coordinates of the atoms weighted according to different weighting schemes (atomic masses, *m*, unitary weights, *u*, van der Waals volumes, *v*, Mulliken atomic electronegativities, *e*, atomic polarizabilities, *p*, and electrotopological indices, *s*). Directional and non-directional WHIM descriptors can be calculated. Directional WHIM descriptors are univariate statistical indices, calculated from the scores of each individual principal component (1, 2, 3), related to molecular size (*L1*, *L2*, *L3*), shape (*P1*, *P2*), symmetry (*G1*, *G2*, *G3*), and density of atom distribution (*E1*, *E2*, *E3*). The non-directional WHIM indices, easily obtained from the directional ones, bear global information about molecular size (*T*, *A*, and *V*), shape (*K*), symmetry (*G*), and density (*D*). WHIM descriptors have been successfully used in developing quantitative structure–activity and structure–property relationships (QSARs and QSPRs) for several sets of compounds and different responses.<sup>38,51–54</sup> Due to their invariance to rotation and translation, WHIM descriptors should allow molecule alignment problems to be overcome, whereas relevant dependence of them upon the molecule conformations can be ruled out due to the rigidity of the PQ derivatives under investigation.

In our study, for each AM1 geometry-optimized PQ molecular model we calculated all 99 WHIM indices (66 directional and 33 non-directional), and subsequently excluded near constant and highly correlated variables through the pretreatment procedures implemented in DRAGON. After variable exclusion (see the methodological section for details), the matrix of WHIM descriptors was reduced to 30 variables, all containing 3-D information on molecular size. A column containing CLOG P values was then appended, and all the data normalized by autoscaling to make the range between variables comparable.

**Principal component analysis (PCA).** PCA is a well known chemometric tool which allows a large table of descriptors to be transformed into a few independent variables (linear combination of original variables)

ordered according to their decreasing variance. In this study, a PCA was performed on the autoscaled data matrix consisting of 31 columns (descriptors) and 56 rows (PQ-containing BzR ligands, categorized into 17 *Ag*, 15 *PA*, 11 *An*, 8 *IA*, and 5 mixed forms). Three principal components taken together accounted for ca. 93.5% of the total variance. The first and the second PCs explained 74.4 and 10.8% of the variance, respectively. A raw Varimax rotation (rotation of scores and related rotation of loadings)<sup>55</sup> in the space of the first three PCs yielded a better variable clustering (not shown) and score plots easier to be evaluated. Figure 6 shows the score plot for the first two varivectors (81.5% retained variance), which illustrates that most of the molecules are spread along two directions of the largest variation. The 8-cyclohexyl PQ derivatives (**2**<sub>3</sub>, **2**<sub>18</sub>, **2**<sub>23</sub>, **2**<sub>29</sub>) are grouped in a small area (middle-bottom side) of the plot, whereas the singleton on the left-hand side is the 8-*n*-butyl PQ **2**<sub>6</sub> bearing a COOCH<sub>3</sub> substituent (the longest one) at the *para* position of the N2-phenyl group.

A close examination of the first versus second varivectors' plot reveals an overlap between the scores of full and partial agonists on the left and most of the antagonists and full inverse agonists on the right-upper corner. The ligands belonging to categories *Ag* and *PA* are mostly spread along the first direction, whereas *An* and *IA* are distributed along a direction nearly orthogonal to that of the full and partial agonists. It is PC1 (74.4%) that mostly explains the variance of the physicochemical properties related to variations of efficacy of compounds in Table 1. The two curves drawn in the plot approximately indicate the boundaries that somehow define areas of highest densities of *Ag* and *PA* (left-bottom) and *An* and *IA* (right-upper corner).

**Classification methods.** Two classification methods, *k*-NN and LDA, were applied to the analysis of 51 compounds, whose in vitro intrinsic activities had been reliably established, in order to find a means able in discriminating among the four categories of efficacy profiles. The whole set was divided into a training set (40 compounds) and a test set (11 compounds), using a random procedure in PARVUS package (details in the methodological section). For LDA, prediction abilities (i.e., the percent of correct assignments to

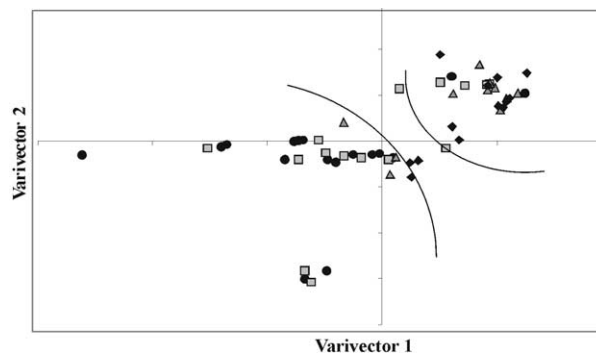


**Figure 6.** Scatter plot of scores of the whole PQ dataset (81.5% retained variance) after raw Varimax rotation. Symbols: *Ag* (●), *PA* (□), *An* (△), *IA* (◆), mixed *IA/An* (○).

efficacy categories) were computed for the PQ derivatives in the training set, using a leave-one-out procedure, and finally assessed by applying the most reliable models for computing the efficacies of the compounds in the test set. Table 2 shows the results obtained with all the categories.

Six out of 31 original variables were selected as the most discriminant ones by stepwise LDA used for feature selection (i.e., selection of the variables producing the greatest Mahalanobis distance between the two closest categories), namely CLOG P, one size non-directional descriptor (*Vs*) and four size directional WHIM descriptors (*L2m*, *L2e*, *L2u*, *L2s*). The global classification ability (i.e., the percentage of molecules correctly in their actual category) was 42.5% by *k*-NN and 77.5% by LDA. However, with the exception of the *Ag* category, the LDA prediction ability was too poor, and a closer examination of the LDA prediction matrix revealed that several misclassifications occurred within the categories *Ag* and *PA* on one side and within the categories *An* and *IA* on the other side, a result somehow reproducing the fuzzy clustering observed in the PCA score plot. We applied to the same matrix PLS-DA (i.e., an extension of the projection methods to Discriminant Analysis),<sup>56</sup> but did not obtain better results (not shown).

The data were then evaluated by pairs of categories, with a special attention paid at the classification and prediction abilities between the contiguous ones (i.e., *Ag/PA*, *PA/An*, *An/IA*). For each subset the most discriminant variables were selected by stepwise LDA (Table 3) and used to compute categories. CLOG P was always retained among the most discriminant variables. The compounds belonging to contiguous and partially overlapped categories (*Ag/PA*, *PA/An*, *PA/IA* and *An/IA*) needed directional WHIM size descriptors to be reasonably well classified and predicted, whereas *Ag* compounds were well distinguished from either *An* and

*IA* ones, based on lipophilicity and total size descriptors. While for a better understanding of the chemical meaning of WHIMs the reader is referred to specialized literature,<sup>52</sup> it is worthy of note that only size descriptors were detected as those mainly representing chemical variation which is somehow related to the efficacy profiles within the examined PQ set. In particular, *L* directional descriptors, which encode information on size in certain molecular regions, were found more or less interrelated among them. The specific information that each descriptor bears is not so easily interpretable, whereas their usefulness in characterizing 3-D molecular topology related to variations in the pharmacological properties were clearly proved by LDA approach.

Global percentages of correct classification and predictions within pairs of categories are reported in a matrix form for training set compounds (Table 4).

The results show fairly good classification and prediction accomplished by LDA of contiguous categories, with the exception of *An/IA* subset. Less good results (not shown) were obtained with *k*-NN. In order to further assess their LDA prediction abilities, the models derived for category pairs were used to calculate efficacy profiles of the compounds in the test set. The results are graphically represented for three models in Figure 7, that shows the separability between contiguous efficacy classes. In Figure 7 the LDA classification in pairs of categories is represented by plotting the differences between the computed discriminant scores; the lines corresponding to the zero scores' difference represent the discriminant surfaces, compounds lying to one side or another of these lines being assigned to the respective classes of intrinsic activities.

As for LDA results obtained with *Ag-PA* subset (plot a), three full agonists (**2**<sub>17</sub>, **2**<sub>18</sub> and **2**<sub>19</sub>) and three partial agonists (**2**<sub>20</sub>, **2**<sub>21</sub> and **2**<sub>25</sub>) are misclassified, whereas three compounds (**2**<sub>14</sub>, **2**<sub>16</sub>, and **2**<sub>27</sub>) almost lie on the discriminant line between the two category profiles (score difference as within  $\pm 0.5$ ). One *PA* (**2**<sub>31</sub>) and one *An* (**2**<sub>35</sub>) are misclassified by LDA as applied to the *PA-An* subset (plot b), and two compounds lie as within  $\pm 0.5$  of the discriminant line (**2**<sub>33</sub> and **2**<sub>36</sub>). The low classification and prediction power (60%) of the LDA as applied to the *An-IA* subset is illustrated by plot c of Figure 7, where the *An* **2**<sub>45</sub> (used as a test set compound) is strongly unpredicted, whereas seven compounds (4 *An* and 3 *IA*) have scores' differences rather close to

**Table 2.** Classification matrix of the four efficacy categories as obtained by LDA on training set (*n* = 40)<sup>a</sup>

Actual category	LDA computed categories				LDA (ability %)		<i>k</i> -NN
	<i>Ag</i>	<i>PA</i>	<i>An</i>	<i>IA</i>	Class.	Pred.	
<i>Ag</i>	12	—	1	—	92.3	84.6	69.2
<i>PA</i>	3	7	1	1	58.3	33.3	16.7
<i>An</i>	1	0	7	1	77.8	55.6	44.4
<i>IA</i>	—	—	1	5	83.3	50.0	33.3

<sup>a</sup>For each category the percent of correct LDA classifications and predictions (leave-one-out procedure) is compared with the results from *k*-NN method.

**Table 3.** Variables selected by stepwise LDA on Training set, as the most discriminant ones between efficacy categories

Subset	Variables retained
<i>Ag/PA</i>	CLOG P, <i>L2s</i> , <i>L2v</i>
<i>Ag/An</i>	CLOG P, <i>Ts</i>
<i>Ag/IA</i>	CLOG P, <i>Tp</i>
<i>PA/An</i>	CLOG P, <i>Tm</i> , <i>L1v</i>
<i>PA/IA</i>	CLOG P, <i>Tm</i> , <i>L2s</i>
<i>An/IA</i>	CLOG P, <i>Au</i> , <i>L1s</i>

**Table 4.** Matrices of global classification and prediction abilities (%) by LDA as applied to subsets of efficacy category pairs in the training set<sup>a</sup>

Actual category	Classification			Prediction		
	<i>PA</i>	<i>An</i>	<i>IA</i>	<i>PA</i>	<i>An</i>	<i>IA</i>
<i>Ag</i>	84.0	91.0	100	84.0	91.0	94.7
<i>PA</i>		81.0	100		81.0	83.3
<i>An</i>			60.0			60.0

<sup>a</sup>Figures along the diagonal represent the LDA discrimination ability among contiguous categories.



zero to be sharply classified. *An* and *IA* remain the ligands more difficult to be distinguished by LDA, most likely because these classes are less populated (11 *An* and 8 *IA*) and poorer of structural information than the *Ag* (17) and *PA* (15) classes.

Despite their limitations, our LDA models, combined with information coming from the lipophilicity scale, allowed the fluoro-containing PQs **2<sub>1</sub>** and **2<sub>2</sub>**, reported herein as novel BzR ligands with antagonistic property,

to be correctly classified. Indeed, PQ derivatives **2<sub>1</sub>** and **2<sub>2</sub>** have CLOG P values of 3.06 and 3.20, respectively, that is a lipophilicity that should characterize them with a profile intermediate between the partial agonism and antagonism. LDA, as applied to *PA–An* subset, with scores' differences of –1.46 and –1.44 for PQs **2<sub>1</sub>** and **2<sub>2</sub>**, respectively, successfully predicted them as antagonists. In addition, the LDA model of *An–IA* once again calculated them as antagonists with very high scores' differences (10.77 and 11.98 for PQs **2<sub>1</sub>** and **2<sub>2</sub>**, respectively).

## Conclusions

In good agreement with previous computational results obtained investigating the pharmacophore of central BzR ligands,<sup>29</sup> our novel 2-phenyl-2,5-dihydropyrazolo[4,3-*c*]quinolin-3-(3*H*)-ones (PQs) exhibited high receptor affinity. In particular, 9-fluoro-2-(2-fluorophenyl)-2,5-dihydro-3*H*-pyrazolo[4,3-*c*]quinolin-3-one (**2<sub>2</sub>**) showed binding affinity in the subnanomolar concentration range and proved to be in vitro a potent antagonist at the benzodiazepine recognition site. This finding not only allowed the three-center HB donor site of the BzR (i.e., the H<sub>2</sub> site located as to between the N-1 nitrogen of the PQ nucleus and the *ortho* position of the N-2-aryl group) to be established as a relevant pharmacophore feature, but also singled out the fluorine-containing PQ derivative **2<sub>2</sub>** as a lead for further developments.

Besides the investigation of the pharmacophore, efforts were made to unravel the structure-efficacy relationships of a large series of PQ derivatives which, depending upon more or less significant structural variation, displayed a shift of intrinsic activities from full (partial) agonism to inverse agonism through antagonism. Such a *continuum* of the efficacy profiles appeared somehow related to a *continuum* of lipophilicity, full agonists being the compounds having the highest log P values and inverse (full) agonists being the less lipophilic compounds. However, the lipophilicity of the ligands could not explain alone the variation of intrinsic activity along the whole series, and to take more structural information into account, we additionally calculated indices of 3-D topology, such as the WHIM descriptors.

Principal component analysis (PCA), a stepwise multivariate method of variable selection and linear discriminant analysis (LDA), progressively applied to a matrix of 51 compounds (divided into a training and test sets of 40 and 11 compounds, respectively) and 31 descriptors, allowed us to quite satisfactorily classify the PQ compounds. Interestingly, LDA, better than the *k*-NN method, distinguished among pairs of efficacy classes and, with the only exception of the *An–IA* model (60% prediction ability), it well (>81%) classified and predicted PQ ligands having contiguous efficacy profiles.

Though applied to one class of structurally related ligands, the pattern recognition methods used in this

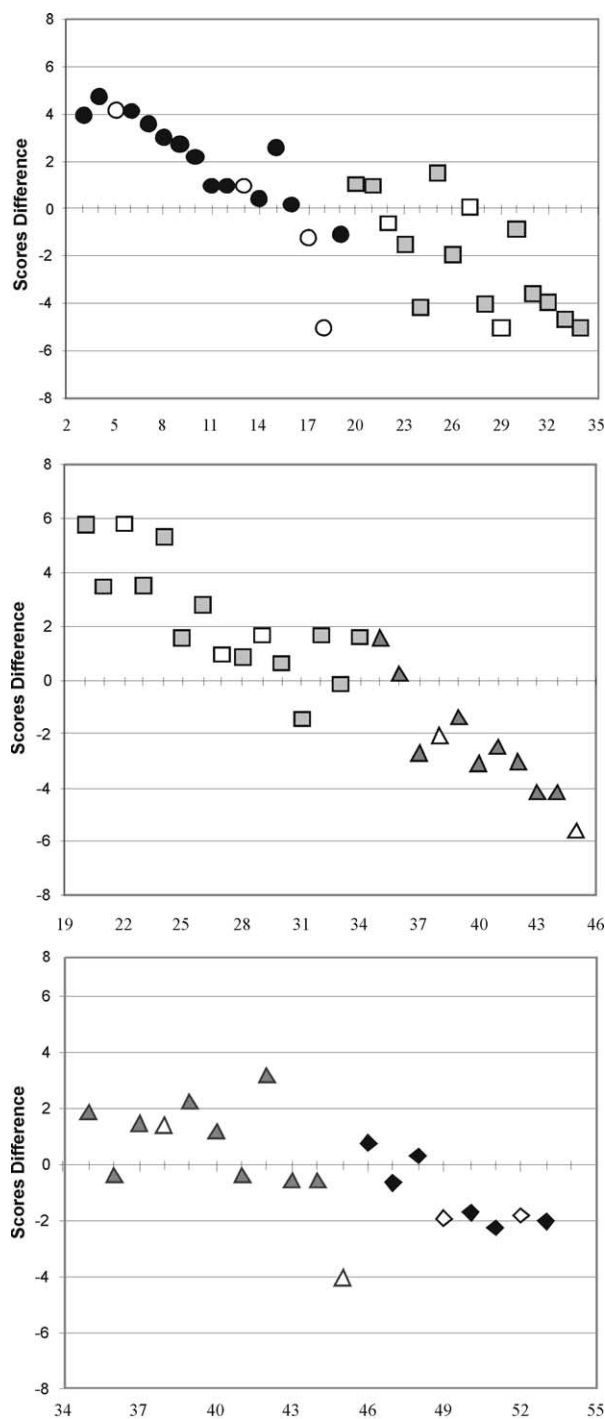


**Figure 7.** Scores' differences computed by LDA on subsets of contiguous efficacy categories: (a) *Ag* (●) and *PA* (◻); (b) *PA* (◻) and *An* (▲); (c) *An* (▲) and *IA* (◆). Empty symbols show the test set compounds. Compound numbering subscripts in abscissa.

study showed potential in extracting discriminant information from a large data matrix and in unveiling structure–efficacy relationships. Multivariate approaches to the analysis of a matrix of physicochemical descriptors proved to be useful in order to distinguish benzodiazepine receptor ligands with different intrinsic activities. The results obtained in this study can usefully complement the existing pharmacophores and 3-D QSAR models based on binding data, allowing the medicinal chemists to rely upon chemometric tools in designing BzR ligands with a given intrinsic activity.

## Experimental

### Chemistry

Melting points were determined on a Büchi B-540 melting point apparatus and are uncorrected. **Elemental analyses** were performed on a Perkin-Elmer elemental analyzer Mod. 240 and the data for C, H, N are within  $\pm 0.40\%$  of calculated values. Spectral analyses (IR and  $^1\text{H}$  NMR) are consistent with the reported chemical structures. IR spectra were determined in Nujol mull on a Perkin-Elmer FT-IR 1600 spectrophotometer.  $^1\text{H}$  NMR spectra were recorded on a AC 200 Bruker instrument. The chemical shifts ( $\delta$ ) are relative to  $\text{Me}_4\text{Si}$  used as internal standard. The following abbreviations were used: s = singlet, d = doublet, t = triplet, dd = double doublet, q = quartet, m = multiplet, u = unresolved, br = broad. The coupling constants  $J$  are measured in hertz. TLC on silica-gel plates (Merck, 60-F<sub>254</sub>) was used for monitoring the reactions. When necessary, column chromatography on silica-gel (Merck, 70–230 mesh and 230–400 mesh ASTH for flash chromatography) was used for isolating and purifying reaction products.

9-Fluoro-2-phenyl-2,5-dihydro-3*H*-pyrazolo[4,3-*c*]quinolin-3-one (**2<sub>1</sub>**), its 2-(2-fluorophenyl) congener (**2<sub>2</sub>**), other four novel 2,5-dihydro-3*H*-pyrazolo[4,3-*c*]quinolin-3-one derivatives (**2<sub>37</sub>**, **2<sub>51</sub>**, **2<sub>52</sub>**, **2<sub>57</sub>**), and one compound already described in patent literature (**2<sub>56</sub>**)<sup>44</sup> were

synthesized during this work by using methods previously reported,<sup>28,29</sup> based on the heterocyclization reaction between the appropriate ethyl 4-chloroquinoline-3-carboxylate and phenylhydrazine (**2<sub>1</sub>**), 2-fluorophenylhydrazine (**2<sub>2</sub>**, **2<sub>37</sub>**), 2-hydrazinopyridine (**2<sub>52</sub>**, **2<sub>56</sub>**, **2<sub>57</sub>**), 2-hydrazinopyrazine (**2<sub>51</sub>**). Physicochemical properties and spectroscopic data of the newly synthesized PQs are summarized in **Tables 5** and **6**, respectively.

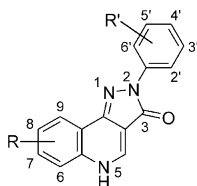
The syntheses of the unknown ethyl 5-fluoro-4-chloroquinoline-3-carboxylate (**1g**), necessary as a starting material for the synthesis of compounds **2<sub>1</sub>** and **2<sub>2</sub>**, and intermediates **d–f** (**Scheme 2**) for its preparation are described in this section.

**Diethyl {(2-bromo-5-fluorophenyl)amino}methylene}malonate (**d**)**. A mixture of 2-bromo-5-fluoroaniline **c** (3.8 g, 20 mmol)<sup>46</sup> and diethyl ethoxymethylenemalonate (4.7 g, 22 mmol) was heated on a steam bath for 16 h. The crude product recrystallized from MeOH–water giving **d** as orange needles (95% yield). Mp 82–83 °C. Anal. ( $\text{C}_{14}\text{H}_{15}\text{BrFNO}_4$ ) C, H, N.  $^1\text{H}$  NMR ( $\text{CDCl}_3$ )  $\delta$  1.34 (t, 6H, 2  $\text{CH}_3\text{--CH}_2\text{O}$ ); 4.29 (q, 4H, 2  $\text{CH}_3\text{--CH}_2\text{O}$ ); 6.73–7.03 (m, 2H); 7.32–7.56 (m, 1H); 8.38 (d, 1H, CH); 11.27 (d, 1H, NH,  $\text{D}_2\text{O}$  exchangeable).

**Ethyl 8-bromo-5-fluoro-4-hydroxyquinoline-3-carboxylate (**e**)**. The intermediate **d** (6.9 g, 19.2 mmol) was dissolved in warm diphenyl ether and the flask was fitted with a Dean–Stark trap to remove EtOH, and the mixture refluxed for 1 h. After cooling at room temperature, diethyl ether was added. The resulting solid, collected by filtration, washed with additional diethyl ether, and purified by crystallization from MeOH gave compound **e** as white needles (79% yield). Mp 198–201 °C. Anal. ( $\text{C}_{12}\text{H}_9\text{BrFNO}_3$ ) C, H, N.  $^1\text{H}$  NMR ( $\text{DMSO-}d_6$ ):  $\delta$  1.29 (t, 3H,  $\text{CH}_3\text{--CH}_2\text{O}$ ); 4.24 (q, 2H,  $\text{CH}_3\text{--CH}_2\text{O}$ ); 7.18 (dd, 1H, H-7); 7.89 (dd, 1H, H-6); 8.35 (s, 1H, H-2); 11.73 (br s, 1H, OH,  $\text{D}_2\text{O}$  exchangeable).

**Ethyl 5-fluoro-4-hydroxyquinoline-3-carboxylate (**f**)**. To a suspension of **e** (1 g, 3.2 mmol) and sodium acetate

**Table 5.** Chemical structures and physicochemical data of the newly synthesized pyrazolo[4,3-*c*]quinolin-3-ones **2**



Compd	R <sub>6</sub>	R <sub>7</sub>	R <sub>8</sub>	R <sub>9</sub>	R <sub>2'</sub>	R <sub>3'</sub>	R <sub>4'</sub>	Mp (°C)	Molecular formula	Cryst. solvent
<b>2<sub>1</sub></b>	H	H	H	F	H	H	H	> 300	C <sub>16</sub> H <sub>10</sub> FN <sub>3</sub> O	EtOH
<b>2<sub>2</sub></b>	H	H	H	F	F	H	H	> 300	C <sub>16</sub> H <sub>9</sub> F <sub>2</sub> N <sub>3</sub> O	EtOH
<b>2<sub>37</sub></b>	H	H	OH	H	F	H	H	> 300	C <sub>16</sub> H <sub>10</sub> FN <sub>3</sub> O <sub>2</sub>	EtOH–H <sub>2</sub> O
<b>2<sub>51</sub></b>	H	H	OCF <sub>3</sub>	H		2-Pyrazin-2'-yl		> 300	C <sub>15</sub> H <sub>8</sub> F <sub>3</sub> N <sub>5</sub> O <sub>2</sub>	EtOH <sup>a</sup>
<b>2<sub>52</sub></b>	H	H	OH	H		2-Pyrid-2'-yl		> 300	C <sub>15</sub> H <sub>10</sub> N <sub>4</sub> O <sub>2</sub>	
<b>2<sub>56</sub><sup>b</sup></b>	H	H	H	H		2-Pyrid-2'-yl		> 300	C <sub>15</sub> H <sub>10</sub> N <sub>4</sub> O	EtOH
<b>2<sub>57</sub></b>	H	H	OCH <sub>3</sub>	H		2-Pyrid-2'-yl		283–285	C <sub>16</sub> H <sub>12</sub> N <sub>4</sub> O <sub>2</sub>	EtOH

<sup>a</sup>Purified by column chromatography (dichloromethane/methanol 18:2).

<sup>b</sup>Ref 46.

**Table 6.**  $^1\text{H}$  NMR and IR spectral data of the newly synthesized compounds<sup>a</sup>

Compd	$^1\text{H}$ NMR ( $\delta$ , ppm; $J$ =Hz)	IR ( $\text{cm}^{-1}$ )
<b>2<sub>1</sub></b>	(DMSO- $d_6$ ): 7.16–7.70 (m, 6H); 8.09 (u d, 1H, H-9); 8.16 (dd, 2H); 8.70 (s, 1H, H-4); 12.87 (br s, 1H, NH, D <sub>2</sub> O exchangeable).	1645 (CO)
<b>2<sub>2</sub></b>	(DMSO- $d_6$ ): 7.30–7.75 (m, 7H); 8.67 (d, 1H, H-4); 12.80 (br s, 1H, NH, D <sub>2</sub> O exchangeable).	1648 (CO)
<b>2<sub>37</sub></b>	(DMSO- $d_6$ ): 7.11 (dd, 1H, H-7, $J_{7-6}$ =8.9, $J_{7-5}$ =2.4); 7.24–7.45 (m, 4H); 7.52–7.59 (m, 2H); 8.57 (s, 1H, H-4); 10.10 (br s, 1H, OH, D <sub>2</sub> O exchangeable); 12.67 (br s, 1H, NH, D <sub>2</sub> O exchangeable).	1647 (CO)
<b>2<sub>51</sub></b>	(DMSO- $d_6$ ): 7.74 (dd, 1H, H-7, $J_{7-6}$ =9.2, $J_{7-9}$ =2.0); 7.89 (d, 1H, H-6, $J_{6-7}$ =9.2); 8.09 (u d, 1H, H-9); 8.51 and 8.62 (2d, 2H, H-(5,6)pyrazinyl); 8.88 (s, 1H, H-4); 9.54 (u d, 1H, H-3 pyrazinyl); 13.08 (br s, 1H, NH, D <sub>2</sub> O exchangeable).	1650 (CO)
<b>2<sub>52</sub></b>	(DMSO- $d_6$ ): 7.13–7.24 (m, 2H, H-5 pyridyl and H-7); 7.54 (d, 1H, H-9, $J_{9-7}$ =2.1); 7.63 (d, 1H, H-6, $J_{6-7}$ =8.9); 7.88 (t, 1H, H-4 pyridyl); 8.23 (d, 1H, H-3 pyridyl, $J_{ortho}$ =8.4); 8.48 (d, 1H, H pyridyl); 8.58 (s, 1H, H-4); 10.20 (br s, 1H, OH, D <sub>2</sub> O exchangeable); 12.88 (br s, 1H, NH, D <sub>2</sub> O exchangeable).	1636 (CO)
<b>2<sub>56</sub></b>	(DMSO- $d_6$ ): 7.21 (td, 1H, H-5 pyridyl); 7.49–7.71 (m, 3H); 7.87 (td, 1H, H-4 pyridyl); 8.19 (u dd, 2H, H-6 and H-3 pyridyl); 8.49 (dd, 1H, H-6 pyridyl, $J_{6-5}$ =4.8, $J_{6-4}$ =1.3) 8.72 (s, 1H, H-4); 12.78 (br s, 1H, NH, D <sub>2</sub> O exchangeable).	1646 (CO)
<b>2<sub>57</sub></b>	(DMSO- $d_6$ ): 7.12–7.23 (m, 2H, H-5 pyridyl and H-7); 7.53 (d, 1H, H-9, $J_{9-7}$ =2.1); 7.63 (d, 1H, H-6, $J_{6-7}$ =8.9); 7.88 (t, 1H, H-4 pyridyl); 8.23 (d, 1H, H-3 pyridyl); 8.48 (d, 1H, H-6 pyridyl); 8.58 (s, 1H, H-4); 10.18 and 12.92 (br s, 2H, OH and NH, D <sub>2</sub> O exchangeable).	1653 (CO)

<sup>a</sup>Mass spectrum: MS:  $m/z$  297 ( $\text{M}^+$ ).

(0.43 g, 3.2 mmol) in 30 mL of glacial acetic acid, 10% Pd/C (0.21 g) was added. The reaction mixture was hydrogenated at room temperature in a Parr apparatus at 35 psi for 10 h, then the catalyst was filtered off and the solution evaporated to dryness. The obtained oil was dissolved in 50 mL of chloroform; the resulting solution, washed with aqueous sodium bicarbonate (15% m/v, 25 mL) and then with water, was dried ( $\text{Na}_2\text{SO}_4$ ) and filtered. After evaporation of the solvent the crude **f** was obtained and purified by crystallization from acetone to give yellow needles (92% yield). Mp 272–274 °C. Anal. ( $\text{C}_{12}\text{H}_{10}\text{FNO}_2$ ) C, H, N.  $^1\text{H}$  NMR (DMSO- $d_6$ ):  $\delta$  1.24 (t, 3H,  $\text{CH}_3\text{--CH}_2\text{O}$ ); 4.17 (q, 2H,  $\text{CH}_3\text{--CH}_2\text{O}$ ); 7.00–7.10 (m, 1H, H-6); 7.50 (dd, 2H, H-6 and H-8); 8.42 (s, 1H, H-2); 11.15 (br s, 1H, OH, D<sub>2</sub>O exchangeable).

**Ethyl 5-fluoro-4-chloroquinoline-3-carboxylate (g).** A mixture of **f** (0.25 g, 1.1 mmol) and  $\text{POCl}_3$  (1.5 mL) was heated in a sand bath at 90 °C for 50 min. After cooling, the reaction mixture was poured into ice-water, neutralized with  $\text{Na}_2\text{CO}_3$ , and extracted with  $\text{Et}_2\text{O}$ . The organic layers, washed with water, were dried on  $\text{Na}_2\text{SO}_4$  and evaporated under reduced pressure. The crude residue, purified by flash chromatography ( $\text{CH}_2\text{Cl}_2$  as the eluent), gave the desired compound **g** as white needles (58% yield). Mp 92–93 °C. Anal. ( $\text{C}_{12}\text{H}_9\text{ClFNO}_2$ ) C, H, N.  $^1\text{H}$  NMR ( $\text{CDCl}_3$ ):  $\delta$  1.44 (t, 3H,  $\text{CH}_3\text{--CH}_2\text{O}$ ); 4.48 (q, 2H,  $\text{CH}_3\text{--CH}_2\text{O}$ ); 7.31 (dd, 1H, H-7); 7.73 (m, 1H, H-6); 7.94 (d, 1H, H-8); 9.02 (s, 1H, H-2).

## Pharmacology

**Chemicals.** [ $^3\text{H}$ ]Flunitrazepam (New England Nuclear, Boston, USA) had a specific activity of 84.3 Ci/mmol and a radiochemical purity >74.6%. [ $^{35}\text{S}$ ]TBPS (New

England Nuclear, Boston, USA) had a specific activity of 72.4 Ci/mmol.

**Animals.** Male Sprague–Dawley rats (Charles River, Como, Italy) with body weights 150–200 g were kept under a 12-h light/dark cycle at a temperature of  $23 \pm 2$  °C and 65% humidity. Upon arrival at the animals facilities there was a minimum of seven days acclimatisation, during which the animals had a free access to food and water. The animals were killed by decapitation and the brains were rapidly removed on ice, the cerebral cortex was dissected out and was used for the measurement of [ $^3\text{H}$ ]Flunitrazepam and [ $^{35}\text{S}$ ]TBPS binding.

Animal care and handling throughout the experimental procedure were performed in accordance with the European Communities Council Directive of 24 November 1986 (86/609/EEC). The experimental protocol were approved by the Animal Ethical Committee of the University of Cagliari.

**[ $^3\text{H}$ ] Flunitrazepam binding.** Cerebral cortices were homogenized in 50 volumes of ice-cold 50 mM Tris–HCl buffer with a polytron PT 10 (setting 5, for 20 s), centrifuged at 48,000g for 10 min and washed one time. The pellet was resuspended in 50 volumes of 50 mM Tris–HCl buffer (pH 7.40) and aliquots of 400  $\mu\text{L}$  tissue homogenate (400–500  $\mu\text{g}$  of protein) were incubated in the presence of [ $^3\text{H}$ ] Flunitrazepam at a final concentration of 0.5 nM, in a total incubation volume of 1000  $\mu\text{L}$ . The compounds were dissolved in DMSO and serial dilutions were made up in DMSO and added in 5- $\mu\text{L}$  aliquots. After 60 min incubation at 4 °C, the assay was terminated by rapid filtration through glass-fiber filter strips (Whatman GF/B). The filters were rinsed with  $2 \times 4$  mL ice-cold 50 mM Tris–HCl buffer with a cell

Harvester filtration manifold (Model M-24, brandel) and transferred in plastic minivials with 3 mL scintillation fluid (AtomLight, New England Nuclear). Six to eight concentrations of the samples in triplicate were used to determine the  $IC_{50}$  values. Non-specific binding was determined as the binding in the presence of 5  $\mu$ M diazepam and was 85–90% of the total binding.

**[ $^{35}$ S]TBPS binding assay.** The cerebral cortex was dissected out and homogenized in 50 volumes of ice-cold 50 mM Tris–citrate buffer (pH 7.4 at 25°C) containing 100 mM  $CaCl_2$  using a Polytron PT 10 (setting 5, for 20 s) and centrifuged at 20,000g for 20 min. The resulting pellet was resuspended in 50 volumes of 50 mM Tris–citrate buffer (pH 7.4 at 25°C) and used for the assay. [ $^{35}$ S]TBPS binding was determined in a final volume of 1000  $\mu$ L consisting of 400  $\mu$ L of tissue homogenate (0.40–0.50 mg protein), 100  $\mu$ L of [ $^{35}$ S]TBPS (final assay concentration of 1 nM), 100  $\mu$ L 2 M NaCl, 100  $\mu$ L of drugs or solvent and buffer to volume. Incubations (25°C) were initiated by addition of tissue and terminated 90 min later by a rapid filtration through glass-fiber filter strips (Whatman GF/B, Clifton, NJ, USA), which were rinsed twice with a 4 mL portion of ice-cold Tris–citrate buffer using a Cell Harvester filtration manifold (model M-24m Brandel, Gaithersburg, MD, USA). Filter bound radioactivity was quantitated by liquid scintillation spectrometry. Nonspecific binding was defined as binding in the presence of 100  $\mu$ M picrotoxin and represented about 10% of total binding. Protein content was determined by the method of Lowry et al.,<sup>57</sup> using bovine serum albumin as a standard.

**Electrophysiological measurements using *Xenopus laevis* oocytes.** Complementary DNAs encoding the human  $\alpha_1$ ,  $\beta_2$ , and  $\gamma_{2L}$  GABA<sub>A</sub> receptor subunits were subcloned into the pCDM8 expression vector (Invitrogen, San Diego, CA, USA). The cDNAs were purified with the Promega Wizard Plus Miniprep DNA Purification System (Madison, WI, USA) and then resuspended in sterile distilled water, divided into portions, and stored at –20°C until used for injection. Stage V and VI oocytes were manually isolated from sections of *X. laevis* ovary, placed in modified Barth's saline (MBS) containing 88 mM NaCl, 1 mM KCl, 10 mM Hepes–NaOH buffer (pH 7.5), 0.82 mM  $MgSO_4$ , 2.4 mM  $NaHCO_3$ , 0.91 mM  $CaCl_2$ , and 0.33 mM  $Ca(NO_3)_2$  and treated with 0.5 mg/mL of collagenase Type IA (Sigma) in collagenase buffer (83 mM NaCl, 2 mM KCl, 1 mM  $MgCl_2$ , 5 mM Hepes–NaOH buffer, pH 7.5) for 10 min at room temperature, to remove the follicular layer. A mixture of GABA<sub>A</sub> receptor  $\alpha_1$ ,  $\beta_2$ , and  $\gamma_{2L}$  subunit cDNAs (1.5 ng/30 nL) was injected into the oocyte nucleus using a 10  $\mu$ L glass micropipette (10–15  $\mu$ m tip diameter). The injected oocytes were cultured at 19°C in sterile MBS supplemented with streptomycin (10  $\mu$ g/mL), penicillin (10 U/mL), gentamicin (50  $\mu$ g/mL), 0.5 mM theophylline, and 2 mM sodium pyruvate. Electrophysiological recordings began approximately 24 h following cDNA injection. Oocytes were placed in a 100- $\mu$ L rectangular chamber and continuously perfused with MBS solution at a flow rate of 2 mL/min at room temperature. The animal pole of oocytes was impaled

with two glass electrodes (0.5–3 M $\Omega$ ) filled with filtered 3 M KCl and the voltage was clamped at –70 mV with an Axoclamp 2-B amplifier (Axon Instruments, Burlingame, CA, USA). Currents were continuously recorded on a strip-chart recorder. Resting membrane potential usually ranged from –30 to –50 mV. Drugs were perfused for 20 s (7–10 s were required to reach equilibrium in the recording chamber). Intervals of 5–10 min were allowed between drug applications. Compounds **2**<sub>1</sub>, **2**<sub>2</sub>, and all the other tested PQ derivatives were dissolved in DMSO then diluted in MBS to a final DMSO concentration of 0.1%. **2**<sub>1</sub> or **2**<sub>2</sub> were first pre applied for 30 s before being co-applied with an  $EC_{5-10}$  (i.e., the concentration of GABA giving 5–10% of the maximal response) concentration of GABA. Intervals of 10–20 min were allowed between drug applications.

### Computational methods

Molecular models of the examined PQ derivatives were built by using the fragment library of SYBYL release 6.7 and their geometries optimized by the AM1Hamiltonian within the suite of MOPAC program.<sup>58</sup> For each test compound 99 WHIM descriptors (66 directional and 33 non-directional) were calculated from the obtained coordinates (\*.mL2 file format) using DRAGON package ver. 2.1.<sup>50</sup> The matrix of WHIM descriptors was preliminarily reduced by excluding constant and highly correlated variables through the pre-treatment procedures suggested by DRAGON. Thus, constant descriptors were excluded by using the option 'near-constant variables' (i.e., descriptors having equal numerical value for all the molecules with the exception of one), whereas multivariate correlation analysis ('Pair correlation' option) allowed us to exclude descriptors intercorrelated with a correlation coefficient equal or higher than the selected threshold value (0.95 in this study). Through such a variable preselection, 31 WHIM descriptors were retained. Furthermore, by carefully analyzing the distribution of the WHIM descriptors retained, we decided to exclude from calculations also the *Elm* variable, because of its poor value distribution. Therefore, finally 12 directional (*L1u*, *L2u*, *L1m*, *L2m*, *L1v*, *L2v*, *L1e*, *L2e*, *L1p*, *L2p*, *L1s*, *L2s*) and 18 non-directional (*Tu*, *Tm*, *Tv*, *Te*, *Tp*, *Ts*, *Au*, *Am*, *Av*, *Ae*, *Ap*, *As*, *Vu*, *Vm*, *Vv*, *Ve*, *Vp*, *Vs*) WHIM descriptors, all containing information about molecular size, were retained. Due to the apparent influence of the hydrophobicity in determining the efficacy profile of the PQ derivatives, we calculated also the octanol–water partition coefficient for each compound by means of CLOG P software,<sup>36</sup> and added it as a further variable column.

Data analysis was carried out by the package PARVUS ver. 3.0.<sup>59</sup> According to their in vitro assessed efficacy profiles, the PQ ligands were subdivided into four categories, i.e., full agonists (*Ag*, 17 compounds), partial agonists (*PA*, 15 compounds), antagonists (*An*, 11 compounds), full inverse agonists (*IA*, eight compounds), and mixed forms (mostly *An-IA*, five compounds). The data matrix of 56 objects (PQ BzR ligands) and 31 descriptors was preliminarily evaluated by PCA. Two classification methods, namely *k*-nearest



neighbors ( $k$ -NN)<sup>39</sup> and linear discriminant analysis (LDA),<sup>40</sup> were then applied to a set of 51 compounds (i.e., those clearly assigned to efficacy categories), divided into a training set (40 compounds) and a test set (11 compounds), by using the program 'Divide' in PARVUS which randomly assigns objects to training and test sets based on given criteria (time randomization option and maximum 25% objects for each category to be placed in the test set for this study).  $K$ -NN is a non-parametric classification method where the classification is based on the relative distance among the objects. For every object, the  $k$  nearest objects are taken into account, and the object is classified into the category with the highest score. In this study, Euclidean distance and  $k = 5$  were used. LDA is a parametric classification method in which the different categories (i.e., efficacy profiles) are supposed to have equal covariance matrices and a different position of the baricenters in the variable hyperspace. For each molecule, the Mahalanobis distance from all the category centroids is computed, and the molecule is classified into the category having the nearest centroid. Before running each LDA, a feature selection (i.e., a selection of the variables having the highest discriminant power) was accomplished by stepwise LDA implemented in PARVUS (to stop selection a 10% maximum increase in Mahalanobis distance between groups and a maximum of variables equal to objects/5 were settled).

### Acknowledgements

The financial support by Italian Ministry for Education Universities and Research (MIUR, Rome, Italy) is gratefully acknowledged. The authors thank Prof. Michele Forina (Dipartimento di Chimica e Tecnologie Farmaceutiche e Alimentari, Genova, Italy) for his careful revision of the chemometric studies and insightful comments.

### Appendix

#### Elemental analysis of synthesized compounds

Compd	C%		H%		N%	
	Calcd.	Found	Calcd.	Found	Calcd.	Found
<b>d</b>	46.69	46.30	4.20	4.25	3.89	3.80
<b>e</b>	45.89	45.78	2.89	2.70	4.46	4.44
<b>f</b>	61.28	61.38	4.29	4.18	5.95	5.90
<b>1g</b>	56.82	56.78	3.58	3.55	5.52	5.50
<b>2<sub>1</sub></b>	68.81	68.68	3.61	3.72	15.05	15.33
<b>2<sub>2</sub></b>	64.65	64.70	3.05	3.15	14.14	14.20
<b>2<sub>37</sub></b>	65.08	65.18	3.41	3.56	14.23	14.38
<b>2<sub>51</sub></b>	51.88	51.90	2.32	2.46	20.17	20.35
<b>2<sub>52</sub></b>	64.74	64.70	3.62	3.70	20.13	20.34
<b>2<sub>56</sub></b>	68.69	68.78	3.84	3.73	21.36	21.22
<b>2<sub>57</sub></b>	65.75	65.53	4.14	4.35	19.17	19.08

### References and Notes

- Bernard, E. A. In *GABA<sub>A</sub> Receptor and Anxiety. From Neurobiology to Treatment*; Biggio, G., Sanna, E., Serra, E., Costa, E., Eds.; Raven: New York, 1995; p 1.
- Barnard, E. A.; Skolnick, P.; Olsen, R. W.; Mohler, H.; Sieghart, W.; Biggio, G.; Braestrup, C.; Bateson, A. N.; Langer, S. Z. *Pharmacol. Rev.* **1998**, *50*, 291.
- Mohler, H.; Fritschy, J. M.; Rudolph, U. *J. Pharmacol. Exp. Ther.* **2002**, *300*, 28.
- Metha, A. K.; Ticku, M. K. *Brain Res. Rev.* **1999**, *29*, 196.
- Sieghart, W. *Pharm. Rev.* **1995**, *47*, 181.
- Takada, S.; Shindo, H.; Sasatani, T.; Chomei, N.; Matsushita, A.; Masami, E.; Kawasaki, K.; Murata, S.; Takahara, Y.; Shintaku, H. *J. Med. Chem.* **1988**, *31*, 1738.
- Shindo, H.; Takada, S.; Murata, S.; Masami, E.; Matsushita, A. *J. Med. Chem.* **1989**, *32*, 1213.
- Wong, G.; Zi-Qiang, G.; Fryer, R. I.; Skolnick, P. *Med. Chem. Res.* **1992**, *2*, 217.
- Fryer, R. I.; Zhang, P.; Rios, R.; Gu, Z. Q.; Basile, A. S.; Skolnick, P. *J. Med. Chem.* **1993**, *36*, 1669.
- Schove, L. T.; Perez, J. I.; Maguire, P. A.; Loew, G. I. *Med. Chem. Res.* **1994**, *4*, 307.
- Fryer, R. I. Ligand Interactions at the Benzodiazepine Receptor. In *Comprehensive Medicinal Chemistry*; Emmett, J. C., Ed.; Vol. 3, Membranes and Receptors; Pergamon: Oxford, 1990; p 539.
- Toja, E.; Tarzia, G.; Barone, D.; Luzzani, F.; Gallico, L. *J. Med. Chem.* **1985**, *28*, 1314.
- Shannon, H. E.; Herling, S. *Eur. J. Pharmacol.* **1983**, *92*, 155.
- Johnson, D. N.; Kilpatrick, B.; Hannaman, P. *Fed. Proc. Fed. Am. Soc. Exp. Biol.* **1986**, *45*, 674.
- Verdoorn, T. A.; Draguhn, A.; Ymer, S.; Seeburg, P. H.; Sakmann, B. *Neuron* **1990**, *4*, 919.
- Crestani, F.; Low, K.; Keist, R.; Mandelli, M.; Mohler, H.; Rudolph, U. *Mol. Pharmacol.* **2001**, *59*, 442.
- Low, K.; Crestani, F.; Keist, R.; Benke, D.; Brunig, I.; Benson, J. A.; Fritschy, J. M.; Rulicke, T.; Bluethmann, H.; Mohler, H.; Rudolph, U. *Science* **2000**, *290*, 131.
- McKernan, R. M.; Rosahl, T. W.; Reynolds, D. S.; Sur, C.; Wafford, K. A.; Atack, J. R.; Farrar, S.; Myers, J.; Cook, G.; Ferris, P.; Garrett, L.; Bristow, L.; Marshall, G.; Macaulay, A.; Brown, N.; Howell, O.; Moore, K. W.; Carling, R. W.; Street, L. J.; Castro, J. L.; Ragan, C. I.; Dawson, G. R.; Whiting, P. J. *Nat. Neurosci.* **2000**, *3*, 587.
- Rudolph, U.; Crestani, F.; Benke, D.; Brunig, I.; Benson, J. A.; Fritschy, J. M.; Martin, J. R.; Bluethmann, H.; Mohler, H. *Nature* **1999**, *401*, 796.
- Takada, S.; Shindo, H.; Sasatani, T.; Chomei, N.; Matsushita, A.; Masami, E.; Kawasaki, K.; Murata, S.; Takahara, Y.; Shintaku, H. *J. Med. Chem.* **1988**, *31*, 1738.
- Shindo, H.; Takada, S.; Murata, S.; Masami, E.; Matsushita, A. *J. Med. Chem.* **1989**, *32*, 1213.
- Wong, G.; Zi-Qiang, G.; Fryer, R. I.; Skolnick, P. *Med. Chem. Res.* **1992**, *2*, 217.
- Fryer, R. I.; Zhang, P.; Rios, R.; Gu, Z. Q.; Basile, A. S.; Skolnick, P. *J. Med. Chem.* **1993**, *36*, 1669.
- Schove, L. T.; Perez, J. I.; Maguire, P. A.; Loew, G. I. *Med. Chem. Res.* **1994**, *4*, 307.
- Zhang, W.; Koehler, K. F.; Zhang, P.; Cook, J. M. *Drug. Des. Discov.* **1995**, *12*, 193.
- Filizola, M.; Harris, D. L.; Loew, G. H. *Bioorg. Med. Chem.* **2000**, *8*, 1799.
- Harris, D. L.; Loew, G. H. *Bioorg. Med. Chem.* **2000**, *8*, 2527.
- Savini, L.; Massarelli, P.; Nencini, C.; Pellerano, C.; Biggio, G.; Maciocco, A.; Tuligi, G.; Carrieri, A.; Cinone, N.; Carotti, A. *Bioorg. Med. Chem.* **1998**, *6*, 389.
- Savini, L.; Chiasserini, L.; Pellerano, C.; Biggio, G.;

- Maciocco, E.; Serra, M.; Cinone, N.; Carrieri, A.; Altomare, C.; Carotti, A. *Bioorg. Med. Chem.* **2001**, *9*, 431.
30. Steiner, T.; Desiraju, G. R. In *The Weak Hydrogen Bond: In Structural Chemistry and Biology*; Oxford University Press: Oxford, 1999.
31. Doyon, J. B.; Jain, A. *Org. Lett.* **1999**, *1*, 183.
32. Deerhovanessian, A.; Doyon, J. B.; Jain, A.; Rablen, P. R.; Sapse, A. M. *Org. Lett.* **1999**, *1*, 1360.
33. Trapani, G.; Franco, M.; Latrofa, A.; Carotti, A.; Genchi, G.; Serra, M.; Biggio, G.; Liso, G. *Eur. J. Med. Chem.* **1996**, *31*, 575, and references therein.
34. Ananthan, S.; Clayton, D. S.; Ealick, E. S.; Wong, G.; Evoniuk, E. G.; Skolnick, P. *J. Med. Chem.* **1993**, *36*, 479.
35. Sanna, E.; Busonero, F.; Talani, G.; Carta, M.; Massa, F.; Peis, M.; Maciocco, E.; Biggio, G. *Eur. J. Pharmacol.* **2002**, *451*, 103.
36. *CLOG P for Windows*, ver. 4.0; Biobyte Corp.: Claremont, CA.
37. Todeschini, R.; Gramatica, P. *Quant. Struct.-Act. Relat* **1997**, *16*, 113.
38. Todeschini, R.; Gramatica, P. *Quant. Struct.-Act. Relat* **1997**, *16*, 120.
39. Massart, D. L.; Dijkstra, A.; Kaufman, L. In *Evaluation and Optimization of Laboratory Methods and Analytical Procedures*; Elsevier: Amsterdam, 1978; p 422.
40. Dillon, W. R.; Goldstein, M. In *Multivariate Analysis, Methods and Applications*; Wiley-Interscience: New York, 1984; p 360.
41. Savini, L.; Massarelli, P.; Pellerano, C.; Fiorini, I.; Bruni, G.; Romeo, M. R. *Farmaco* **1993**, *48*, 65.
42. Savini, L.; Massarelli, P.; Corti, P.; Pellerano, C.; Bruni, G.; Romeo, M. F. *Farmaco* **1993**, *48*, 1675.
43. Yokoyama, N.; Ritter, B.; Neubert, A. D. *J. Med. Chem.* **1982**, *25*, 337.
44. Yokoyama, N. (Ciba-Geigy A.-G.), Eur. Pat. Appl. 22,078, 7 Jan. 1981; *Chem. Abstr.* **1981**, *95*, 7278s.
45. Higuchi, J.; Fujisawa, M.; Yokoyama, Y.; Yagi, M. *J. Photochem. Photobiol. A: Chem.* **1999**, *124*, 53.
46. Hutchinson, I.; Chua, M.-S.; Browne, H. L.; Trapani, V.; Bradshaw, T. D.; Westwell, A. D.; Stevens, M. F. G. *J. Med. Chem.* **2001**, *44*, 1446.
47. Squires, R. F.; Casida, J. E.; Richardson, M.; Saedrup, E. *Mol. Pharmacol.* **1983**, *23*, 326.
48. Gee, K.; Lawrence, L. J.; Yamamura, H. I. *Mol. Pharmacol.* **1986**, *30*, 218.
49. Concas, A.; Serra, M.; Atsoggiu, T.; Biggio, G. *J. Neurochem.* **1988**, *51*, 1868.
50. Todeschini, R.; Consonni, V.; Pavan, M. *DRAGON*; ver. 2.1; Talete srl: Milan, Italy.
51. Todeschini, R.; Lasagni, M.; Marengo, E. *J. Chemom.* **1994**, *8*, 263.
52. Todeschini, R.; Gramatica, P.; Provenzani, R.; Marengo, E. *Chemom. Intell. Lab. Syst.* **1995**, *27*, 221.
53. Todeschini, R.; Vighi, M.; Provenzani, R.; Finizio, A.; Gramatica, P. *Chemosphere* **1996**, *32*, 1527.
54. Todeschini, R.; Bettiol, C.; Giurin, G.; Gramatica, P.; Miana, P.; Argese, E. *Chemosphere* **1996**, *33*, 71.
55. Forina, M.; Armanino, C.; Lanteri, S.; Leardi, R. *J. Chemom.* **1988**, *3*, 115.
56. Sthåle, L.; Wold, S. *J. Chemom.* **1987**, *1*, 185.
57. Lowry, O.; Rosebrough, N.; Lewis Farr, A.; Randall, R. *J. Biol. Chem.* **1951**, *193*, 265.
58. Stewart, J. J. P. *J. Comput.-Aided Mol. Des* **1990**, *4*, 1.
59. Forina, M.; Lanteri, S.; Armanino, C. *Q-PARVUS 3.0, An Extendible Package of Programs for Data Explorative Analysis, Classification and Regression Analysis*; Dipartimento di Chimica e Tecnologie Farmaceutiche e Alimentari: Genova, Italy (Web address: <http://parvus.unige.it>).